33RD CONGRESS
OF THE INTERNATIONAL COUNCIL
OF THE AERONAUTICAL SCIENCES
STOCKHOLM, SWEDEN, 4-9 SEPTEMBER, 2022

ICAS 2022 SWEDEN

TESTING AND MODELLING OF A DUCTED FAN MOTOR FOR UAV APPLICATIONS

Björn-Ole Schröder[1], Pedro J. González[2] & Flávio J. Silvestre[3]

[1,2,3]Department of Flight Mechanics, Flight Control and Aeroelasticity, Technical University of Berlin, 10587 Berlin, Germany

Abstract

This paper presents a process to generate numerical models of electric ducted fans for a flying aeroelastic demonstrator. In this research, a testbed was built and integrated into a data acquisition system to perform static and dynamic tests. A wind tunnel test was conducted. A model of thrust in function of the incoming air stream and the throttle position was obtained via polynomial interpolation. The resultant motor model has a high correlation with the measured data and it is easy to integrate into the UAV flight dynamics model.

Keywords: Electric ducted fan, motor modeling for flight dynamics, experimental setups, motor characterization.

1. Introduction

Today's aviation is confronted with many challenges, one of them being global warming and its contribution to it. To achieve more sustainable and environmentally friendly aviation the Advisory Council for Aeronautics Research (ACARE) developed the flightpath 2050 supported by representatives of industry, airlines, and several institutes. With regards to the goal of "Protecting the environment and the energy supply" a reduction of 75% in CO2 emissions and 90% in NOx emissions in comparison to "typical new aircraft in 2000" is aimed for [1].

There are many variables that can contribute to achieve mentioned goals, in general they can be: aerodynamic efficiency improvement and increased efficiency of propulsion and structural weight reduction. A high aspect ratio wing increases the aerodynamic efficiency due to reduction of induced drag and therefore can reduce the fuel consumption significantly. Further these high aspect ratio wings often go with composite materials to achieve weight savings and ensure structural integrity. Thus the aeroelastic behaviour becomes nonlinear due to the high flexibility which is yet not well understood, carrying a risk for aeroelastic instabilities like flutter [2]. Another risk is the coupling between rigid body and structural dynamics [3]. This phenomenon can reduce the validity of commonly used flight dynamics models and conventional controllers, deteriorating the handling qualities or even compromising the safety of the aircraft [4], [5].

To better understand these interactions, the TU-Berlin's Chair of Flight Mechanics, Flight Control and Aeroelasticity in cooperation with the German Aerospace Center's Institute of Aeroelasticity had designed the TU-Flex. The aim of the TU-Flex is to capture in-flight data to validate flight dynamics models of very flexible aircraft and therefore better describe the aeroelastic behaviour of very flexible wings. The flying demonstrator has a configuration that permits tracing conclusions applicable to a new generation of these more efficient and eco-friendly transport and commercial airliners. Within the features of this platform are interchangeable high aspect ratio wings with different levels of flexibility and complex rigid-body and structural-dynamics measurement system coupled with a flight computer. The pilot and control commands to the motors come from this system. To reduce the environmental impact, the operational risk of the aircraft and the model uncertainty pertaining fuel consumption, the designer selected two ducted-fan electric motors as propulsion system of the TU-Flex.

These motors were usually made for the RC model, therefore, the exact performance and endurance data is not available. Normally, these information are rare and for commercial off the shelf motors nearly non-existent. As interest in small unmanned aerial vehicles (SUAVs) has increased in recent years in both industry and academia, so has the need for performance data. For the TU-Flex flight dynamics model, it is necessary to have an accurate model of the motor, able to run fast and to be easily integrated with the rest of the aircraft model. At the same time, it is necessary to confirm that the selected motors are capable to fulfill the performance requirements of the aircraft. The TU-Flex's drag polar and therefore the thrust requirement is shown in Fig. 1. The other restriction is that the aircraft should take off maximum in 60 m.

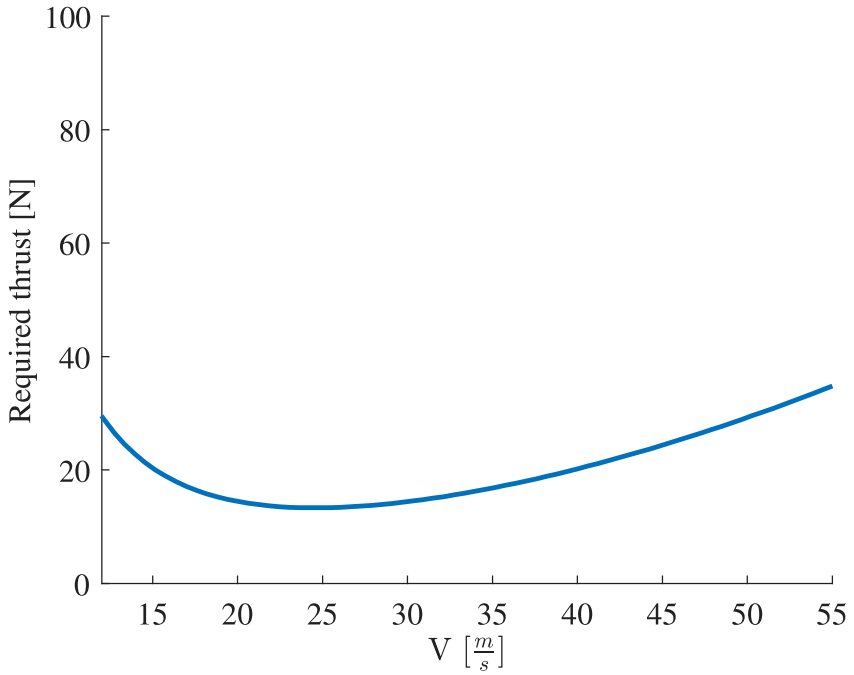

Figure 1 – TU-Flex thrust requirements

The required thrust was calculated, but the truly available thrust is still unknown. Further the throttle position to achieve these thrust ratings is unknown and no data of the dynamic behaviour is available. Therefore, the objective of this study is to measure the thrust of two electric ducted fans as a function of speed and commanded throttle setting. The acquired data is then used to create a model of the motor for the nonlinear simulation of the TU-Flex. The performance of the battery will also be monitored, so first assumptions about endurance can be evaluated. To achieve this, the test bed and the procedure was designed. The tests were conducted at the Aerodynamics department of the TU-Berlin. Then, the data needs to be reduced and processed to generate the flight mechanics model of the motors. Derived from the TU-Flex flight envelope, the velocity range of interest is between $15\frac{m}{s}$ to $45\frac{m}{s}$ and the accuracy of the model is aimed for $\pm$0.5 N.

The use and testing of ducted fans and propellers date back to 1960 when the NASA investigated the use of ducted propellers for vertical take-off and landing (VTOL) applications. These researches mainly focused on the transition of vertical to horizontal flight and the related change in angle of attack [6], [7], [8]. Since test beds for EDFs in forward flight are not as common as test beds for propeller testing, different papers with the subject of performance tests have been considered to gain an overall impression of existing setups. After all an adaption of the inputs will be made to match the project specific targets.

In the research of Brandt and Selig (2011), the thrust and torque of a propeller engine were measured and coefficients as well as general efficiency were calculated in consideration of several correction factors [9]. The airflow velocity ranged from $0\frac{m}{s}$ up to the speed of 0 resulting force, also known as the windmill state. The measurement of the thrust was completed through a pendulum T-shaped structure that pivoted about two flexural pivots while being constrained by a load cell outside of the

tunnel [9]. To reduce drag on the structure a fairing was applied to it. Torque was measured by a torque transducer placed behind the motor housing inside the wind tunnel. The RPM were measured by a photo reflector and the air flow velocity was measured using a pitot tube in combination with two differential pressure transducers for different speed ranges. A 200W electric motor and a gearbox system drove the propellers controlled via a servo checker. The authors suggested two test modes. Either the propeller speed is kept constant while sweeping the tunnel speed or a constant wind speed is set and the throttle is changed. They went with mode one for their propeller performance analysis. After the data reduction, wind tunnel and velocity corrections were applied for wall and blockage effects. The following coefficients were calculated allowing the comparison of different propellers:

$$J = \frac{V}{nD} \quad (1) \qquad c_T = \frac{T}{\rho n^2 D^4} \quad (2) \qquad c_P = \frac{P}{\rho n^3 D^5} \quad (3) \qquad \eta = J\frac{c_T}{c_P} \quad (4)$$

In the end, the coefficients over the advance ratio were presented. However, the purpose of the current work is to provide a function that allows the flight control computer (FCC) to obtain the thrust with only the throttle input and the true airspeed as input parameters. Hence coefficients, the advance ratio and the rotor efficiency are less practicable. Moreover the calculation would consume further computing capacity. Since the overall objective of the TU-Flex is the investigation of the aeroelastic behaviour, computing resources should be conserved.
The thrust model of Guimaraes Neto et al. (2021) with air flow velocity and throttle setting as input parameters was used for the ITA-X-HALE [10]. The project faced the same issue of missing performance data. This research proposed a more direct modelling approach to create the thrust model for the aircraft using wind tunnel experiments. Further details on how these tests were conducted is given in the report by Gonzalez (2015) [11]. For the test, the motors were powered by a ground supply with the voltage set at the average steady-state voltage provided by the aircraft batteries in flight. The thrust was measured with a sting balance and was recorded along with the RPM. The throttle was recorded with the data acquisition and transmission system (DATS). The test was run in the range of $10\frac{m}{s}$ to $20\frac{m}{s}$ with $2\frac{m}{s}$ as the increment and throttle of 15% to 95%. The final thrust model was plotted in Fig. 2.The surface was obtained through piece-wise linear interpolation of the data points.

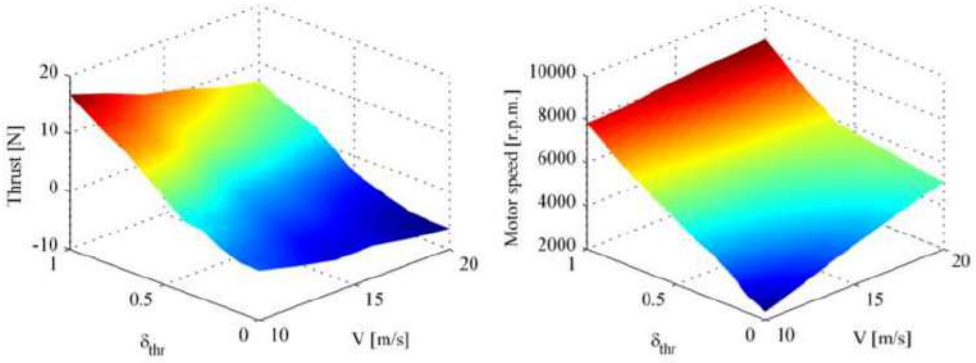

Figure 2 – Thrust and motor speed plotted over throttle and velocity [10]

2. Experimental Setup

2.1 Test Section

The tests were performed at the open jet wind tunnel 2 of the TU Berlin located in the institute for aerospace engineering. The maximum velocity to be reached is $30\frac{m}{s}$. The operating Reynolds number is 2.7×10^6. A rectifier and two fine screens in the agitation chamber provide a turbulence intensity of 0.56%. The test section is 400 mm x 400 mm of size. The wind tunnel is shown in Fig. 3.

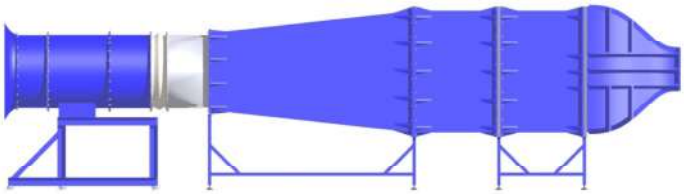

Figure 3 – Open jet wind tunnel 2 of the TU Berlin

The electric ducted fan that is the subject of this work is the Schübeler DS-51-DIA HST, pictured in Fig 4. Two engines were considered; EDF Nr.1 is rotating clockwise and EDF Nr.2 is rotating counterclockwise. In the following the results will refer to in this order.

Figure 4 – Schübeler DS-51-DIA HST

The data provided by the supplier is listed in Table 1. The YGE Aureus 135 electronic speed controller

Table 1 – Technical data of Schübeler DS-51-DIA HST

Characteristic	Value
motor configuration	DSM4335-950
diameter	93 mm
total weight	590 g
airflow exit velocity	82-98 $\frac{m}{s}$
rpm range	29300-34800
power input	2.4-4.1 kW
efficiency	70%-71%
maximum static thrust	41 N - 59 N

(ESC) was recommended for usage. The engine was powered by the same LiPo batteries that will be used inflight. Those were the SLS Quantum 5000mAh 12S1P 44.4V 40C. To control the ESC a STM32F407 Discovery board was programmed to generate the PWM signal.
A test bed was designed for the experiment. The aim was a measurement accuracy of $\pm$0.5 N. Therefore a sensor with a high accuracy and a nominal force of up to 200N was desired. Further the build volume should be kept small to allow a positioning close to the EDF inside the test section. This idea was later abandoned to prevent electro magnetic induction by the engine. The sensor used

was the KD24s s-type force sensor provided by ME-Messsysteme. The amplifier GSV-2TSD-DI was used due to its RS232 interface and a 24bit resolution. Since the sensor had to be placed outside of the test section, a support structure was designed, that passes the thrust underneath the ground plate, where the sensor was placed. Therefore, the motor mount was fixed to four linear ball bearings that slide on two rods underneath the plate, as shown in Fig. 5. In this way the front face area was also minimized in the test section. A fairing needed to be added, since the minimal safety distance could not be kept at the test facility. After the assembly, the entire structure was put vertically and then calibrated with dead weights. This calibration resulted in an accuracy of $\pm$ 0.5 N. The entire assembly and the force transfer mechanism are pictured in Fig. 5 and Fig.6.

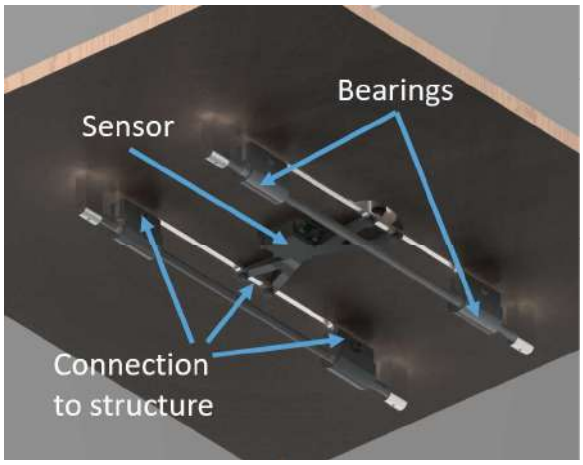

Figure 5 – Sliding mechanism

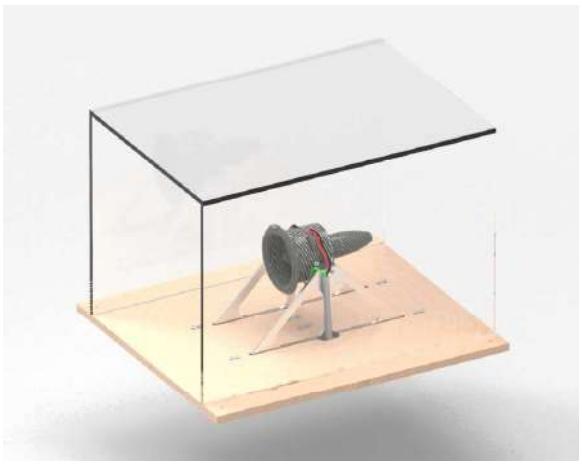

Figure 6 – Test section

2.2 Data acquisition system

To record the synchronized data, a dSpace PX10 box was used with the DS1006 Processor board and several digital and analogue I/O boards [12]. The dSpace was controlled with the ControlDesk, a software installed on a host PC that is connected to the dSpace via an optical interface. Further a Matlab/Simulink library is available to configure the simulation model and compile it to the dSpace. Starting with the velocity, the dynamic pressure was measured using a Pitot tube and a Kal84. The output was an analogue voltage signal that allowed the calculation of the velocity with given temperature and pressure. The force was measured with the s-type force sensor. Its signal was amplified and filtered by the amplifier. The amplifier was then connected via a RS232 interface to the DS1006 processor board. The communication protocol was provided by the supplier and implemented in the Simulink model. Since the amplifier can be set to output the force, no further calculation was necessary. The last signal to be measured was the PWM control variable. Therefore the PWM output of the STM32 board was split and connected to the DS4004 HIL digital I/O board. Again this was implemented in the Simulink model which was then compiled and finally run on the dSpace. The entire data acquisition system is pictured in Fig. 7. To monitor and record the test runs, the ControlDesk software was used. The data sets were saved in .mat format for data post processing.

3. Test procedure

Analogue to the operating velocity of $15\frac{m}{s}$ to $45\frac{m}{s}$, the testing was aimed to be done in this range. However, due to the wind tunnel operational limits, the maximum possible wind speed to be tested was approximately $30\frac{m}{s}$. To achieve the function for thrust, a matrix of discrete measurement points was set up with entries of the resulting force while every column and row was associated with a certain level of the throttle and the airspeed of the wind tunnel. For this work, the two test modes of Brandt and Selig (2011) were considered [9]. Since the power supply for the motors was no external DC supply, the batteries would have faced a very high load using the first mode. The wind speed would have to be varied slowly to allow the engine to adapt and have a steady thrust measurement. After all, a test run in this mode, at 100% throttle, could have lead to the batteries overload. Thus the first

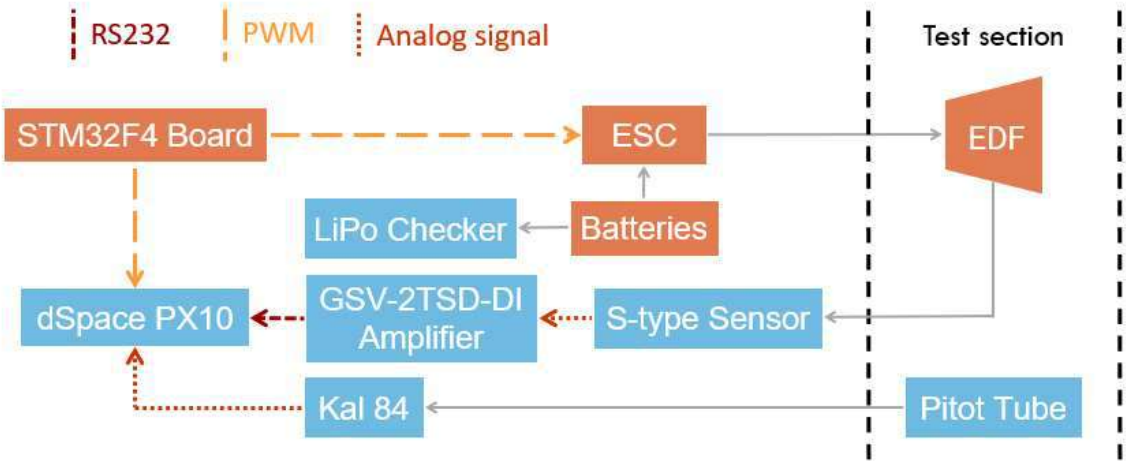

Figure 7 – Scheme of data acquisition set up

mode was not feasible. The second mode consisted on setting a constant wind speed and varying the throttle of the motor. With this mode the wind speed could be set as desired and then the engine would be cycled through the different throttle settings. Afterwards, corrections for induced velocity and other effects could be applied if necessary. Also a static thrust measurement was included for the take-off conditions of the airplane. The motors were set to 100% and then decreased with an increment of 10% until there was no more thrust produced. Since the function needed to be extrapolated to make up the low maximum wind speed, the increment from $20\frac{m}{s}$ to $30\frac{m}{s}$ was set to $2.5\frac{m}{s}$ to allow the extrapolation with reasonable accuracy. In addition the static measurement with $0\frac{m}{s}$ and an airspeed slightly below the take off speed with $15\frac{m}{s}$ were tested too. To further gather data on the battery endurance and to approximate the power consumption of the EDF, three additional test runs were planned. The throttle was set to 50% and 75% and the test was run at $30\frac{m}{s}$ until a fully charged battery was discharged. Another test was done with 15 N of thrust, to simulate one motor inoperative flight condition. Finally, there were two last tests to determine the dynamic response behaviour. Therefore a sine sweep was generated as input for the throttle with 25% to 75% amplitude and up to a frequency of 5 Hz. This was done for $0\frac{m}{s}$ and $30\frac{m}{s}$. To later correct the thrust by considering the drag produced by the test structure, a velocity sweep was performed on the structure without the EDF mounted. The test section and the EDF during a test run are shown in Fig. 8 and Fig. 9.

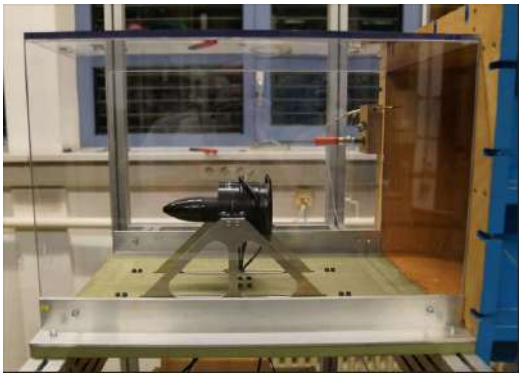

Figure 8 – EDF during a test run

Figure 9 – Build test section

4. Results

For every test run, there was a data file generated. Since there was noise in the thrust measurement due to vibrations, the raw data needed to be post processed. First outliers were filtered. Therefore, a moving mean was formed that included 2000 values equivalent to 2 seconds. Outliers were then defined as elements more than the threshold of 1.5 of local standard derivation. These elements were then replaced by the center value of the mean area. Since the data was still noisy, it was then smoothed. The method used was again the moving median because it is less sensitive to the outliers, that could not be filtered. The moving window was fitted to each of the data sets. Afterwards significant change points were identified automatically and the segment means were calculated. The raw and the post processed data for the test run of $30\frac{m}{s}$ is pictured in Fig. 10. Starting at 100% of throttle, the mean values were then transferred to the thrust matrix. This was done automatically for every air speed. Afterwards the thrust was corrected for the structural drag.

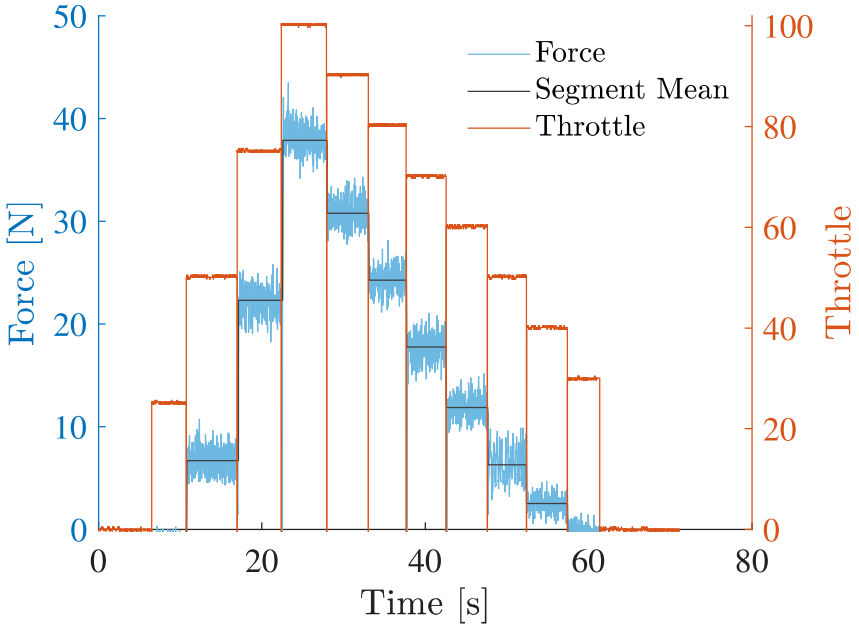

Figure 10 – Exemplary data post processing at 30 $\frac{m}{s}$

A polynomial of 2x2 degree was then fitted to the matrix with $R^2 = 0.9968$. Figure 11 and Fig. 12 show the resultant function. It is visible for both engines that the resulting thrust of the test runs with $30\frac{m}{s}$ is above the trend. Since the test run at $30\frac{m}{s}$ was the last run for each engine, in both cases the battery needed to be changed due to low voltage. This caused the slight increase in thrust.
The maximum static thrust is 55.12 N and 55.41 N with uncorrected atmosphere. At an airspeed of $30\frac{m}{s}$ it decreases to 40.02 N and 41.76 N. The extrapolated values for $40\frac{m}{s}$ are 35.26 N and 37.76 N. The difference in thrust may be caused by different atmospheric conditions.
Now that the thrust was known, a correction for the airspeed due to blockage was considered. According to Fitzgerald (2007) the Glauert correction is recommended for propeller testing and will be considered in this case to [13]. The corrected velocity V' is calculated with Eqn. 5. Considering the cross-sectional area of the fan A and the windtunnel C, the thrust T, the density ρ and the measured airspeed V.

$$\frac{V'}{V} = 1 - \left(\frac{\frac{T}{\rho C V^2}}{2 \cdot (1 + 2 \cdot \frac{T}{\rho A V^2})^{\frac{1}{2}}}\right) \tag{5}$$

With the biggest deviation at the highest velocity of 30 $\frac{m}{s}$ the deviation is less than 4% and 1 $\frac{m}{s}$ absolute value. Thus the blockage effect was neglected for the modelling.

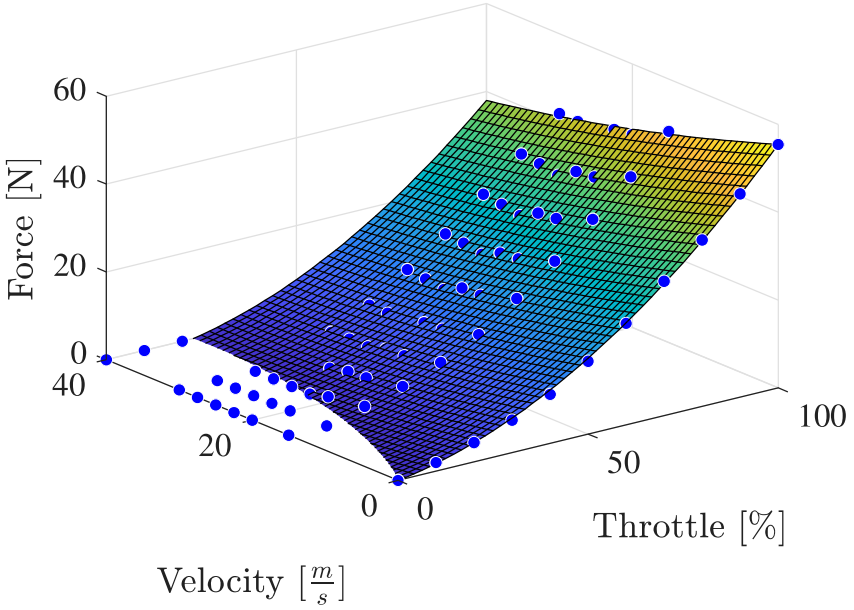

Figure 11 – Thrust model for EDF no.1

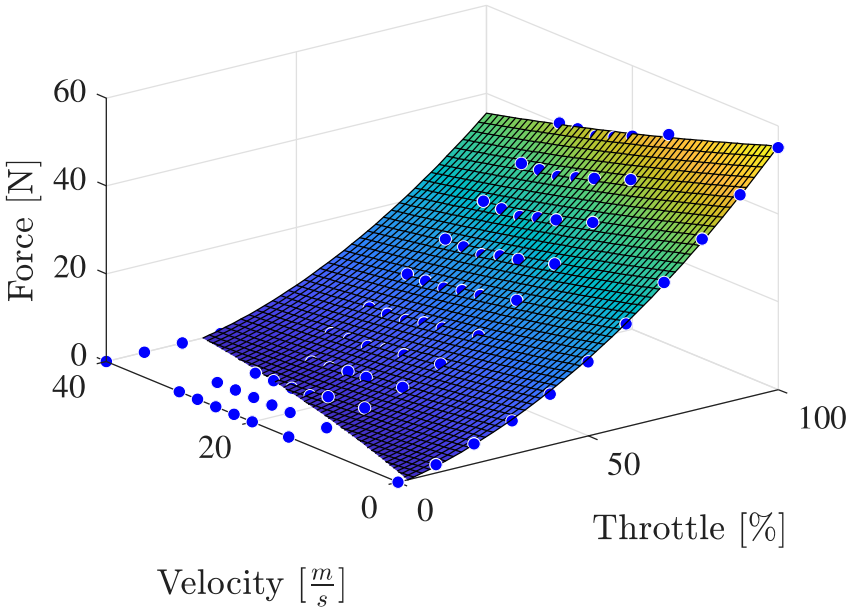

Figure 12 – Thrust model for EDF no.2

The results of the sine sweep test at $30\frac{m}{s}$ are pictured in Fig. 13 and Fig. 14. The data was normalized by the maximum value of each force and throttle. The EDF responds nearly instantaneous and follows the input signal. It is visible in Fig. 13 that the minimum of each period starts to raise at 75 s. Further the maxima start fluctuating at 80 seconds. The equivalent frequency at 75 s is 2 Hz. Both engines show a fast response behaviour and a pilot coupling in thrust seems very unlikely. Nevertheless, a good characterization of the motor delay is necessary for control design. Figure 14 shows the delay between throttle command and resulting force. The mean delay is 0.05 s which was considered in the final model.

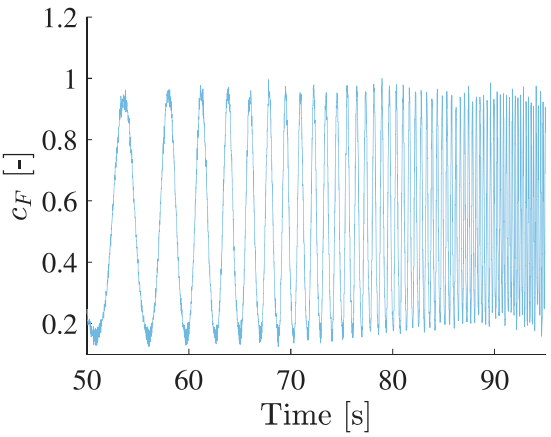

Figure 13 – Sine sweep of EDF no.2

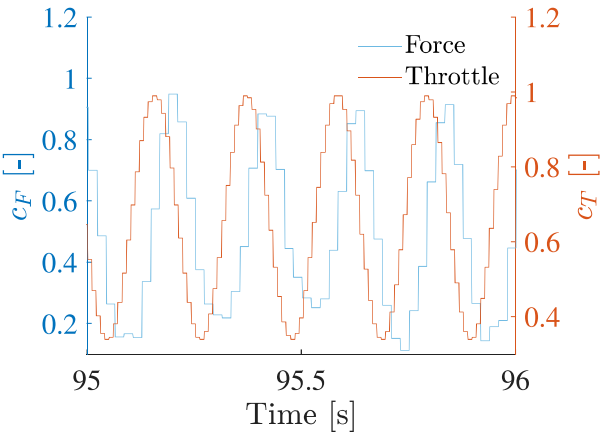

Figure 14 – End of sine sweep

The overall aim of this research was to provide the TU-Flex with a realistic thrust model that can then be used for the flight dynamics simulations. Therefore the functions of the fitted surfaces of Fig. 11 and 12 needed to be implemented in Simulink. It is possible to write a function including the polynomial of the fitted surface with all the coefficients coded hard into Simulink. However to be flexible for future corrections of voltage of the batteries or further improvements a more elegant approach was preferred. The solution was to directly implement the fitted objects containing the polynomial. Since the implementation is not as simple as loading a variable from the workspace, a function handle was created which is then called by the interpreted function block in the Simulink model. This was done for both models which were then added to get the resulting thrust. Lastly the previously determined delay of 0.05 s was added. The final model is pictured in Fig. 15.

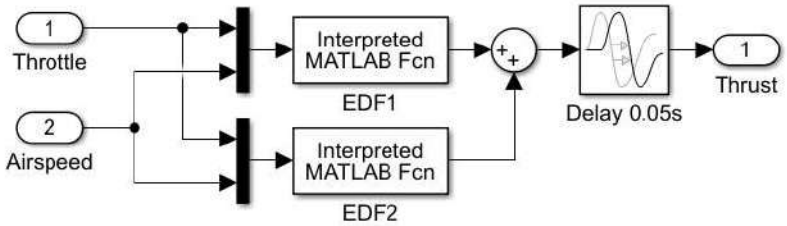

Figure 15 – Simulink model

To validate the results of the modelling method in general and therefore compare it with recorded data, a separate model without the drag correction was made for each engine. In Fig. 16 and Fig. 17 the throttle commands were used as input for this model. The results were plotted with the actual resulting force. The test run at $0\frac{m}{s}$ shows precise alignment. However at $30\frac{m}{s}$ the aforementioned battery change leads to slightly increased thrust than calculated, especially at 60%-90% throttle position. The average error due to these circumstances is -0.73 N and $+0.61$ N for EDF Nr.1 and -0.45 N and $+0.50$ N for EDF Nr.2. Overall the model matches the data as desired for all velocities and thrust levels.

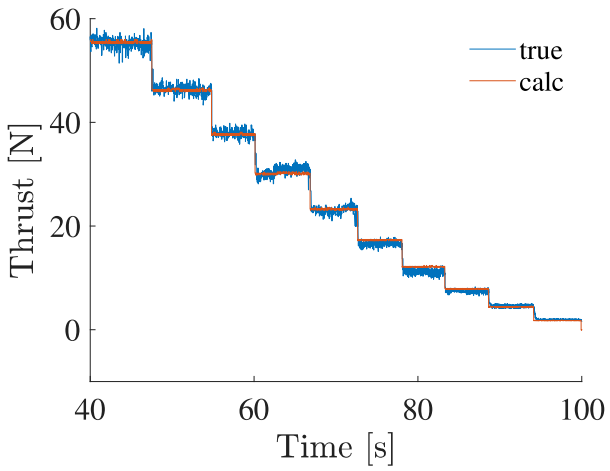

Figure 16 – EDF 1 at $0\frac{m}{s}$

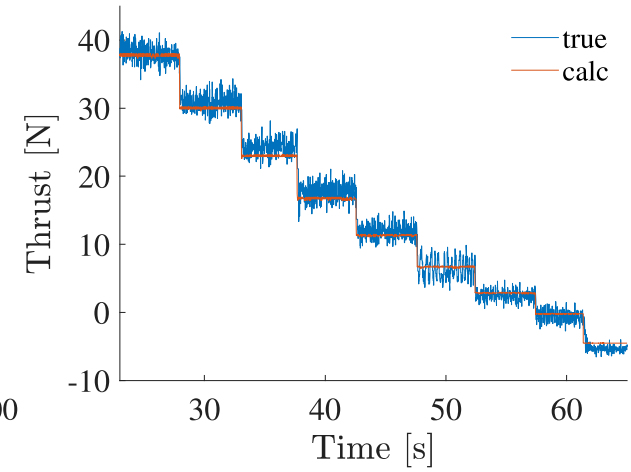

Figure 17 – EDF 2 at $30\frac{m}{s}$

The thrust requirements of the TU-Flex were defined in Section 1. After combining the two models, the available thrust is known. The results are pictured in 18. With a flight envelope of $15-45\frac{m}{s}$ the engines can be operated at a minimum of 41% of Throttle position. First endurance tests have shown that a single battery last nearly up to 10 min of operating time at 50% of throttle. Taking into account that the launch consumes a significant amount of energy and that each motor is powered by two batteries, a flight time of 15 minutes can be estimated. Further in case of one EDF inoperative, the second EDF is supposed to provide enough thrust to return and land safely. At 56% of throttle the lowest required thrust can be achieved. Another restriction was that the aircraft is supposed to take off within 60 m of runway. With the current thrust model a take off within 55.5 m is possible, so all requirements were met.

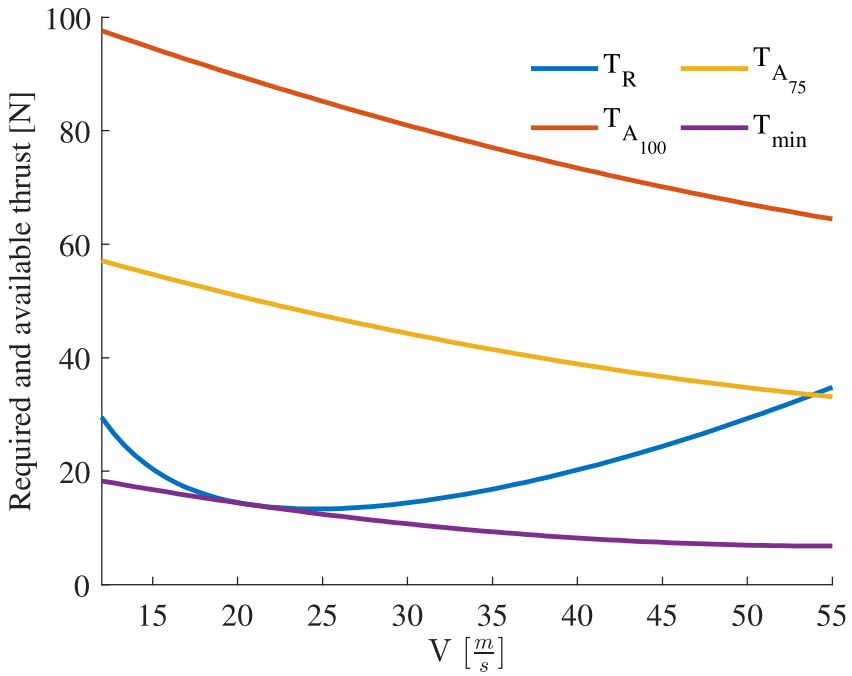

Figure 18 – Required and available thrust for different throttle settings and velocities

5. Conclusion

In this research, a process for generating numerical models of two electric ducted fans was presented. First, a testbed was built. To achieve this, multiple constructions for propeller and jet engine testing were reviewed. Usually, thrust is modeled over the advance ratio, but since this value is not an available input for the model, only the force, throttle, and airspeed were measured and recorded. Therefore an S-type force sensor and a pitot tube were used. Wind tunnel tests were then conducted. The airspeed was set constant and the throttle was varied for all velocities, resulting in similar high power consumption. This way excessive stress to the batteries due to high and constant power consumption at high throttle levels was avoided. The data was then post-processed to remove outliers and noise. The resulting thrust was averaged and the values were extracted in dependency on the airspeed and throttle level. After the correction of the structural drag and consideration of airspeed corrections, a model was obtained via polynomial interpolation. The resultant motor model has a high correlation with the measured data and is easy to integrate into the UAV flight dynamics model.

In addition to the model itself, these motors are being considered for use in the TU-Flex aeroelastic demonstrator. This aircraft has a set of requirements for the available thrust and assumptions derived from them. Assumptions about the flight duration were confirmed and are likely to be exceeded. Also, the take-off restriction of a 60 m runway is met. Moreover, in the case one engine is inoperative, the second engine can still provide enough thrust to keep the demonstrator airworthy. After all the EDFs are considered suitable for the TU-Flex.

6. Acknowledgements

The authors would like to thank Andreas Salecker and his team in the *Institute für Luft und Raumfahrt* (ILR) workshop, who built all the parts of the test stand. The authors acknowledge Dr. Thomas Grund and Christopher Ruwisch for the support at the ILR - wind tunnel test facilities and in the setting up process of the DSpace and data acquisition system.

7. Contact Author Email Address

The authors' contact e-mails are: b.schroeder@campus.tu-berlin.de, pedro.gonzalez@dlr.de and flavio.silvestre@tu-berlin.de

8. Copyright Statement

References

[1] E. Commission, D.-G. for Mobility, Transport, D.-G. for Research, and Innovation, *Flightpath 2050 : Europe's vision for aviation : maintaining global leadership and serving society's needs*. Publications Office, 2011.

[2] C. Howcroft, D. Calderon, L. Lambert, M. Castellani, J. E. Cooper, M. H. Lowenberg, and S. Neild, "Aeroelastic modelling of highly flexible wings," in *15th dynamics specialists conference*, 2016, p. 1798.

[3] F. J. Silvestre, A. B. G. Neto, R. M. Bertolin, R. G. A. da Silva, and P. Paglione, "Aircraft control based on flexible aircraft dynamics," *Journal of Aircraft*, vol. 54, no. 54, pp. 262–271, 2016.

[4] D. Drewiacki, F. J. Silvestre, and A. B. Guimarães Neto, "Influence of airframe flexibility on pilot-induced oscillations," *Journal of Guidance, Control, and Dynamics*, vol. 42, no. 7, pp. 1537–1550, 2019.

[5] P. J. González, F. J. Silvestre, M. d. F. V. Pereira, Z. Y. Pang, and C. E. Cesnik, "Loop-separation control for very flexible aircraft," *AIAA Journal*, vol. 58, no. 9, pp. 3819–3834,, 2020.

[6] P. F. Yaggy and K. W. Goodson, *Aerodynamics of a tilting ducted fan configuration*. National Aeronautics and Space Administration, 1961.

[7] K. W. Goodson and K. J. Grunwald, *Aerodynamic characteristics of a powered semispan tilting-shrouded-propeller VTOL model in hovering and transition flight*. National Aeronautics and Space Administration, 1962, vol. 981.

[8] K. J. Grunwald, *Division of Aerodynamic Loads on a Semispan Tilting-ducted-propeller Model in Hovering and Transition Flight: Kalman J. Grunwald and Kenneth W. Goodson*. National Aeronautics and Space Administration, 1962.

[9] J. Brandt and M. Selig, "Propeller performance data at low reynolds numbers," in *49th AIAA Aerospace Sciences Meeting including the New Horizons Forum and Aerospace Exposition*, 2011, p. 1255.

[10] A. B. Guimarães Neto, G. C. Barbosa, J. A. Paulino, R. M. Bertolin, J. S. Nunes, P. J. González, F. L. Cardoso-Ribeiro, M. A. Morales, R. G. da Silva, F. L. Bussamra *et al.*, "Flexible aircraft simulation validation with flight test data," *AIAA Journal*, pp. 1–20, 2021.

[11] P. J. González, "Evaluation of the gt 2215 engine as a replacement for the pj s 1200," *Instituto Tecnológico de Aeronáutica LNCA Internal Report*, 2015.

[12] dSpace GmbH, *dSPACE-Manual for Modular System Based on D1006*. dSpace GmbH, 2021, vol. Release 2021-B.

[13] R. E. Fitzgerald, *Wind tunnel blockage corrections for propellers*. University of Maryland, College Park, 2007.